

Towards an Automated Pipeline to Create Patient Specific 3D LV Geometry Models of Patients with Mitral Annular Disjunction

Gabriel Balaban¹, Eivind Westrum Aabel², Margareth Ribe², Anna Isotta Castrini², Kristina Haugaa², Mary M Maleckar¹

¹ Computational Physiology Department, Simula Research Laboratory, Oslo, Norway)

² Department of Cardiology, Oslo University Hospital, Oslo, Norway

Abstract

Mitral annular disjunction (MAD) is characterized by an abnormal insertion of the posterior mitral leaflet on the atrial wall. Despite its often subtle presentation, the presence of MAD can be a warning sign of future ventricular tachycardia (VT) and sudden cardiac death (SCD), as recent studies have shown association among MAD-related imaging metrics and VT/SCA. Nevertheless, the precise mechanisms leading to VT/SCD in patients with MAD are poorly understood. A comprehensive 3D shape analysis of the left ventricles (LV) of patients with MAD may provide further insight and help to elucidate mechanisms. Towards this end, we created a patient-specific 3D LV geometry modelling pipeline for patients with MAD, to enable future morphological studies based on cardiac short axis magnetic resonance imaging (MRI).

We applied our pipeline to derive personalized 3D LV geometries in a cohort of 69 patients with MAD originating from Oslo University Hospital. To demonstrate the utility of our pipeline, we performed a statistical comparison of the dominant modes of shape variation of our patient cohort with records of prior arrhythmia.

1. Introduction

Mitral annular disjunction (MAD) is a structural abnormality of the mitral annulus associated with mitral leaflet prolapse. It is characterized by an abnormal insertion of the posterior mitral leaflet on the atrial wall. It was first recognized in a comprehensive autopsy study in 1986 in the context of floppy mitral valves [1]. MAD then remained a medical curiosity until 2010, when it was noticed in routine echocardiography studies. In particular, Carmo et al. [2] noted a link between the amount of valve plane disjunction in MAD, and the occurrence of non-sustained ventricular tachycardia (NSVT) during Holter monitoring. Later, an arrhythmic variant of MAD was identified by Deigaard et al. [3], based on the observation of severe

ventricular arrhythmic events and sudden cardiac death in patients with MAD but no concomitant valvular disease. Most notably, myocardial fibrosis was noticed in the papillary muscles of patients with MAD and severe arrhythmias [3], indicating the presence of tissue damage and remodelling related to the abnormal valvular mechanics, as the papillary muscles connect directly to the mitral valves via the chordae tendineae.

In order to further investigate the link between MAD and arrhythmia, we constructed a 3D LV geometry analysis pipeline, and tested it on MRI data from a cohort of 69 patients with MAD. We hypothesized that tissue damage and remodelling related to severe arrhythmias in MAD patients would be detectable via bulk shape changes of the left ventricle. This was inspired by a previous study in dilated cardiomyopathy patients [4], which showed a link between left ventricular shape changes and subsequent arrhythmia.

2. Methods

MRI data and processing: Our imaging dataset consisted of standard short axis gadolinium contrast enhanced magnetic resonance images of 69 patients from Oslo University Hospital [5], with signs of mitral valve prolapse and mitral annular disjunction (Fig 1). Two patients were excluded due to severe slice misalignments, leaving 67 patients in the study. Nine of these patients had a history of prior ventricular tachycardia (VT) or aborted sudden cardiac death (aSCD), whereas 12 had a history of non-sustained ventricular tachycardia (NSVT).

LV epicardial and endocardial contours were marked in each image slice using a semi-automated neural network based technique (Segment, Medviso), and were exported for further processing. Three points on the septum were marked on the most basal slice of each patient, (Fig 2C) to determine an LV-RV axis (Fig 2D) for the purpose of model alignment.

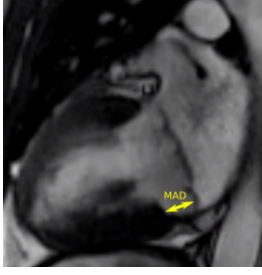


Figure 1. Long-axis cardiac MRI image of a patient with mitral annular disjunction in systole. The yellow arrow highlights the gap between the ventricular wall and the mitral valve attachment point

Semi-automated LV Geometry Modelling Pipeline: The main components of our LV geometry modelling pipeline are displayed in Fig 2. To build personalized LV geometries (Fig 2B), all MRI derived contours were placed in a Euclidean coordinate system, with the x-y directions aligning with the image slices, and with z representing the out-of plane long axis direction. Next, a template mesh was fitted to each patient’s LV epicardial and endocardial contours in a three step procedure, consisting of slice shift correction, template mesh generation, and registration.

Slice shift correction was performed by fitting a 2nd order polynomial (apical-basal axis) to the centre of the LV blood pool in each short axis slice. All contours were then shifted so that their centres aligned with the apical-basal axis, to correct for minor slice shifts due to breathing [6].

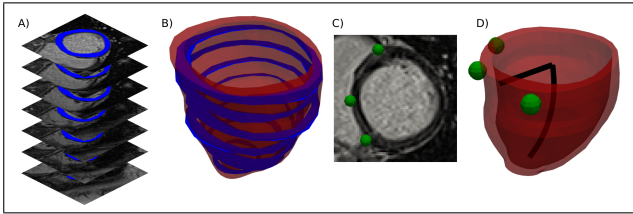


Figure 2. Semi-automated pipeline to create patient specific 3D LV geometry models of patients with MAD. A) Short axis MRI slices with the myocardium labelled in blue. B) Fitted LV geometry model obtained by registration of a template mesh to the MRI derived myocardial contours. C) Three manually selected landmarks used to obtain a consistent model orientation. D) Final LV model with two orientation axes (apical-basal and RV).

Next an ellipsoidal template mesh was generated for each patient. This template was parametrized by w_t, z_c, s_{xy}, s_z , the wall thickness, the z-coordinate of the ellipsoid centre, and ellipsoid scaling parameters in Cartesian coordinates respectively. The following optimization problem was solved to fit the template parameters

$$\min f(s_{xy}, s_z, z_c, X_{epi}) + f(s_{xy} - w_t, s_z - w_t, z_c, X_{endo}) \quad (1)$$

where f is given by the ellipse equation

$$f(s_{xy}, s_z, z_c, X) = \frac{S_{xy}}{s_{xy}^2} + \frac{(z - z_c)^2}{s_z^2} - 1, \quad (2)$$

where

$$S_{xy} = (x - x_c(z))^2 + (y - y_c(z))^2, \quad (3)$$

and $X = (x, y, z)$, and X_{endo}, X_{epi} are the endocardial and epicardial contour points respectively. Also, $x_c(s), y_c(z)$ are the x - y coordinates of the apical-basal axis at level z. The template fitting problem (1) was solved using Scipy’s SLSQP solver.

All ellipsoidal template geometries were implemented using the Visualization Tool Kit (VTK), using 84 linear hexahedral elements, with a thickness of 1 element through the myocardial wall. The dimensions of these geometries were specified by the optimized template parameters. Next, each template was cut off at the most basal contour ($z = 0$), and warped by the previously calculated apical-basal axis, so that the template blood pool centres aligned with the corresponding image-based endocardial contour centres.

The final step in our 3D patient-specific LV geometry modelling pipeline was registration of the template mesh to the MRI endocardial and epicardial contours. This was accomplished by optimizing quadratic B-spline transformations via the software Elastix [7]. A 3D B-spline transform was built by solving 2D slice-by slice problems. Each 2D problem consisted of binary image registration, where the fixed image was formed by binarizing the ellipsoidal geometry at a slice with constant z-value corresponding to a single MRI image in the SAX stack. This image was registered to the moving image, formed by marking the myocardium as 1 and everything else as 0 in the corresponding MRI slice. For each slice-level, a mean squares metric with a bending energy regularization function was minimized with 250 iterations of an adaptive stochastic gradient descent optimizer. To improve the stability of the registration process, a regularization strength of 1.0 was set, along with an image pyramid schedule of 2,1, that is a preliminary registration at half resolution, followed by a registration at full resolution. Once completed, the slice level 2D B-spline transformations were assembled into a single global 3D transformation. This ensured that the transformed mesh remained present at all levels of the MRI image stack, as the global 3D transformation function did not include any shift in the z-direction. The code for the creation of the patient-specific LVED geometries was implemented in Python, and is publicly available via Zenodo [8] (<https://doi.org/10.5281/zenodo.7125360>).

Statistical Analysis All patient 3D LV geometry models were aligned into a common space using their apical-basal and RV axes (Figure 2D). The coordinates of all the mesh points were then gathered into a single patient times coordinate matrix and decomposed using principle component analysis to generate modes of variation. A Mann-Whitney

u test was used to compare LV shape mode content between patients who suffered an VT/aSCD versus those who had no prior history of arrhythmia.

3. Results

We successfully constructed patient specific 3D LV geometries for all 67 patients in our cohort. The mean distance between the image contours and the mesh (Hausdorff distance error) was less than 1.0 mm for all patient meshes, whereas the maximum Hausdorff distance error was less than 6.2 mm. We display the resulting meshes in Figure 3, along with the location of the myocardium within each corresponding MRI image slice. We note that the 3D LV geometries fit closely to the image-based myocardial slices.

We decomposed all of the 67 patient-specific left ventricular end-diastolic (LVED) geometries into modes of variation, which are displayed in Figure 4. Together, the first five shape modes (M1-5), accounted for 93.2% of the variation in LVED shape. The first mode M1 combines variance in the long-axis dimension and sphericity of the LV shape, with the positive direction giving a longer long-axis and more spherical LV. The second mode M2 represents a lengthening of the LV chamber along the long-axis, whereas modes M3-M4 represent tilting of the LV, with M4 also containing a change in basal diameter. Finally mode M5 represents changes in the short-axis dimension. All of our LV geometries and PCA modes are publicly available [9].

We compared the mode contents of patients with VT/aSCD ($n = 9$) versus patients with no prior arrhythmia ($N = 46$). The results are presented in Figure 5, and show that the mode M1 content was higher in the patients with VT/aSCD versus those with no prior arrhythmia ($P = 0.04$). Note that the patients who suffered NSVT ($n = 12$) were not included in this analysis.

4. Discussion

Our analysis highlights a subtle LVED shape difference in the patients with MAD and VT/aSCD, as compared to those with MAD and no history of major arrhythmia. This finding shows that arrhythmic MAD is more than just a valvular disease, and is mostly likely driving a remodelling process in the LV myocardium. This is corroborated by previous evidence of LV fibrosis in this patient group [3]. Our detected shape difference could be related to ventricular remodelling as a downstream consequence of arrhythmia, or a driver of the arrhythmia which persisted until the MRI were acquired. Further research with prospective arrhythmia outcome data and larger cohorts is required to corroborate our findings.

Fully automated pipelines have been recently deployed to construct personalized ventricular geometry meshes for



Figure 3. Anterior view of patient specific left-ventricular shape models of 67 patients with mitral annular disjunction. The corresponding location of the myocardium within each MRI image slice is marked in white for the sake of comparison.

biophysical simulation [10] and shape analysis [11]. These pipelines are based on the use of neural networks to automatically segment the epicardial and endocardial contours in both the LV and RV. Given that such automated segmentation technologies are becoming more commonly available, the full automation of our pipeline is a relatively straightforward step. A more complex issue is the automated segmentation and 3D modelling of the valve plane and papillary muscles, which would be of great interest for future studies into MAD and other valvular diseases. We invite future researchers to address these key issues.

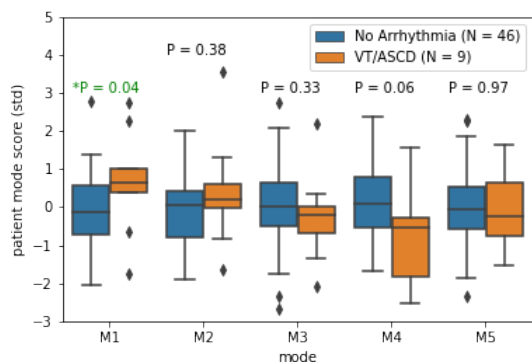


Figure 5. Statistical comparison of LVED shape mode content between patients who suffered an VT or ASCD versus patients who had no record of prior arrhythmia. The difference in mode M1 is statistically significant ($P = 0.04$). Patients with a record of NSVT ($n = 12$) were excluded from the analysis.

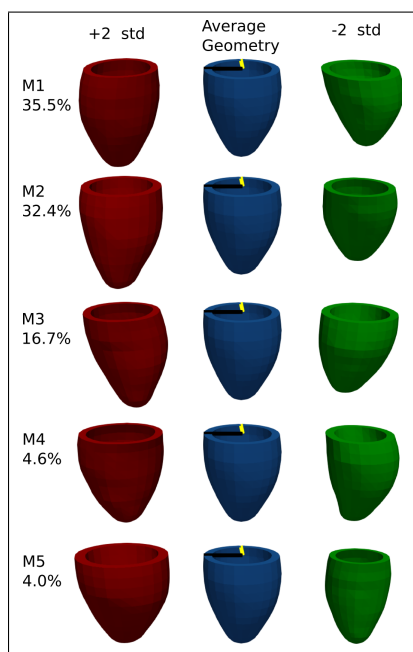


Figure 4. The first five modes of LVED shape variation in our MAD patient cohort. The percentages underneath the mode labels (M1-M5) indicate the percentage of total shape variance explained by each mode. The ± 2 std geometries represent variations along each mode with respect to the average geometry.

Acknowledgments

We thank the Norwegian Research Council for funding this research via a grant to the PROCARDIO Centre for Cardiological Innovation.

References

- [1] Hutchins GM, Moore GW, Skoog DK. The association of floppy mitral valve with disjunction of the mitral annulus fibrosus. *New England Journal of Medicine* 1986; 314(9):535–540.
- [2] Carmo P, Andrade MJ, Aguiar C, Rodrigues R, Gouveia R, Silva JA. Mitral annular disjunction in myxomatous mitral valve disease: a relevant abnormality recognizable by transthoracic echocardiography. *Cardiovascular Ultrasound* 2010;8(1):1–7.
- [3] Dejgaard LA, Skjølsvik ET, Lie ØH, Ribe M, Stokke MK, Hegbom F, Scheirlynck ES, Gjertsen E, Andresen K, Helle-Valle TM, et al. The mitral annulus disjunction arrhythmic syndrome. *Journal of the American College of Cardiology* 2018;72(14):1600–1609.
- [4] Balaban G, Halliday BP, Hammersley D, Rinaldi CA, Prasad SK, Bishop MJ, Lamata P. Left ventricular shape predicts arrhythmic risk in fibrotic dilated cardiomyopathy. *EP Europace* 2022;24(7):1137–1147.
- [5] Aabel EW, Chivulescu M, Dejgaard LA, Ribe M, Gjertsen E, Hopp E, Hunt TE, Lie ØH, Haugaa KH. Tricuspid annulus disjunction: novel findings by cardiac magnetic resonance in patients with mitral annulus disjunction. *JACC Cardiovascular Imaging* 2021;14(8):1535–1543.
- [6] Swingen C, Seethamraju RT, Jerosch-Herold M. An approach to the three-dimensional display of left ventricular function and viability using MRI. *The International Journal of Cardiovascular Imaging* 2003;19(4):325–336.
- [7] Klein S, Staring M, Murphy K, Viergever MA, Pluim JP. Elastix: a toolbox for intensity-based medical image registration. *IEEE Transactions on Medical Imaging* 2009; 29(1):196–205.
- [8] Balaban G. Iyshaper: Cardiac left ventricle 3D geometry creation tool from short axis MRI, September 2022. URL <https://doi.org/10.5281/zenodo.7125360>.
- [9] Balaban G. URL <https://doi.org/10.6084/m9.figshare.21230939.v1>.
- [10] Banerjee A, Camps J, Zacur E, Andrews CM, Rudy Y, Choudhury RP, Rodriguez B, Grau V. A completely automated pipeline for 3D reconstruction of human heart from 2D cine magnetic resonance slices. *Philosophical Transactions of the Royal Society A* 2021;379(2212):20200257.
- [11] Corral Acero J, Schuster A, Zacur E, Lange T, Stiermaier T, Backhaus SJ, Thiele H, Bueno-Orovio A, Lamata P, Eitel I, et al. Understanding and improving risk assessment after myocardial infarction using automated left ventricular shape analysis. *JACC Cardiovascular Imaging* 2022; 15(9):1563–1574.

Address for correspondence:

Gabriel Balaban
 Simula Research Laboratory, Kristian Augusts gate 23, 0164,
 Oslo, Norway
 gabrib@simula.no